

A robust damping droop control based on energy reshaping

Opracowanie metody sterowania zwrotnego w celu poprawy stabilności i wydajności sieci energetycznej

Abstract. This work contributes to advancing the understanding and application of grid-forming inverters for power sharing in microgrids. The focus is to develop a new framework including droop control methods for enhancing the stability and performance of the grid. Advanced droop controllers, based on interconnection and damping assignment passivity-based control (IDA-PBC) methodology, will be proposed, including dual integrators. These controllers demonstrate very good performance in voltage and current stabilization and help to overcome problems of stability, local oscillations, and transient behaviour under islanded mode. The proposed methodology allows smooth and flexible energy distribution, thus approaching a very strong solution for microgrid management. MATLAB simulations are employed to validate the performance and reliability of the proposed control strategies.

Streszczenie. Niniejsza praca przyczynia się do poszerzenia wiedzy i zastosowania falowników typu grid-forming w celu współdzielenia mocy w mikrosieciach. Głównym celem jest opracowanie nowej struktury, obejmującej metody sterowania zwrotnego (droop control), w celu poprawy stabilności i wydajności sieci. Zaproponowano zaawansowane regulatory zwrotne, oparte na metodzie sterowania pasywnego z przypisaniem tłumienia i połączeń (IDA-PBC), w tym podwójne integratory. Regulatory te wykazują bardzo dobre właściwości w stabilizacji napięcia i prądu oraz pomagają przewyżnić problemy związane ze stabilnością, lokalnymi oscylacjami i zachowaniem przejściowym w trybie wyspowym. Zaproponowana metoda umożliwi płynną i elastyczną dystrybucję energii, stanowiąc tym samym bardzo skuteczne rozwiązanie w zarządzaniu mikrosieciami. Symulacje w środowisku MATLAB zostały wykorzystane do potwierdzenia wydajności i niezawodności zaproponowanych strategii sterowania.

Keywords: Distributed generator, droop control, microgrid, island, grid-forming

Słowa kluczowe: Generator rozproszony, sterowanie opadaniem napięcia, mikrosieć, tryb wyspowy, formowanie sieci

Introduction

Due to the increasing electrical loads that need to be powered, especially in isolated areas, microgrids are frequently employed to meet consumer demands. They typically include PV panels, wind turbines, and other distributed energy sources [1, 2]. A microgrid comprises several distributed generators connected in parallel to enhance power production while improving reliability, flexibility, and service continuity.

However, microgrids still have problems with stability because of factors such as power-sharing during island mode operation. The solutions for regulating these systems can be divided into grid-following and grid-forming approaches, where each one has many types of controls, such as droop control, which fits within the grid-forming control. It ensures active and reactive power distribution, eliminates circulating currents between multiple distributed generators, and mitigates transient and permanent circumstances during unexpected switching of loads and production units [3].

Droop control has been widely developed as conventional droop, transient droop, droop control with virtual impedance [4], and droop control with two integrators [5].

This study provides a general control strategy for an autonomous microgrid consisting of a droop control with two integrators with voltage and current regulation based on interconnection and damping assignment passivity-based control (IDA-PBC) for systems represented in the Port Hamiltonian (PCH) form. This control provides high voltage quality within the standalone microgrid and corrects active and reactive power allocation among generators and loads. The Hamiltonian function reflects the energy of the physical system. This strategy allows us to quickly and easily develop generic, modular control that maintains the system's stability by directing energy toward the chosen equilibrium point. This stability is assured without needing any intervention from the other local controllers, even when the microgrid is reconfigured [6].

The proposed control approach tackles the inherent issues of circulating currents and provides a scalable and modular solution that boosts the operating capabilities of MGs. By using detailed simulations and comparing different controllers, this study shows how advanced a droop control technique could make independent microgrids much more reliable and improve their performance.

The paper is organized into five sections. The system's structure and modelling are presented in Part II. The inverter's control techniques, including two types of droop control and types of VSI control, are described in section III. Section IV presents the simulation results for the different control combinations. Finally, section V contains the conclusion of the study.

Distributed Generator

The main parts of a microgrid system always include distributed generators (DG), which mean DC sources, inverters, and LC filters. That is connected to loads, and an impedance transmission line connects them. In this system, a control allows it to regulate the voltage at each DG's output and adjust the power-sharing between them. The internal model of each DG is based on the relations between current and voltage equations across the filter, which can be described in abc frame. V_{Cabci} is shown as the voltage at the capacitor, and i_{Labci} is the three-phase current at the point of common coupling (PCC), where V_{abci} and i_{abci} are the voltage and the current at the output of the inverter, respectively. Where (i) represents the number of the inverter [7].

$$(1) \quad L_i \frac{di_{abci}}{dt} = v_{abci} - v_{Cabci}$$

$$(2) \quad C_i \frac{dv_{abci}}{dt} = i_{abci} - i_{Labci}$$

Transformed into the synchronously rotating frame (SRF).

$$(3) \quad L_i \frac{di_{di}}{dt} = L_i \omega_i i_{qi} + v_{di} - v_{cdi}$$

$$(4) \quad L_i \frac{di_{qi}}{dt} = -L_i \omega_i i_{di} + v_{qi} - v_{cqi}$$

$$(5) \quad C_i \frac{dV_{cdi}}{dt} = i_{di} - i_{Ldi} + C_i \omega_i v_{cqi}$$

$$(6) \quad C_i \frac{dV_{cqi}}{dt} = i_{qi} - i_{Lqi} - C_i \omega_i v_{cdi}$$

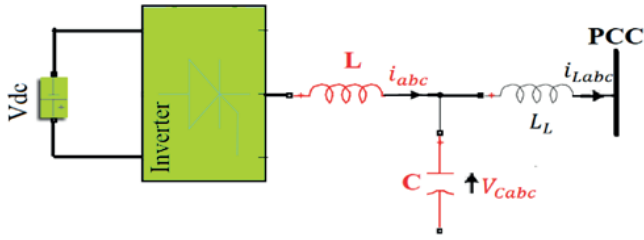


Fig. 1. Main circuit schematic diagram. [5]

Inverter Controls

The control strategies applied to the inverter are mitigated through a two-stage approach, incorporating internal control and primary control. The proposed solutions involve droop control as the primary control and voltage source inverter (VSI) as the secondary stage, representing internal control.

Voltage source inverter

The voltage source inverter control ensures that each distributed generator outputs a sinusoidal voltage waveform. System stability is maintained, static mistakes are rectified, and disturbances are disregarded. The literature proposed techniques and control strategies to operate each scattered generating unit independently for the best performance. The number of control loops used, the nature of the control (linear or nonlinear), and other parameters, such as proportional–integral (PI) controllers, all influence the outcome [5], [8].

$$(7) \quad i_{d}^* = P_v(s)(v_{cd}^* - v_{cd}) + i_{ld} + C\omega v_{cq}$$

$$(8) \quad i_{q}^* = P_v(s)(v_{cq}^* - v_{cq}) + i_{lq} + C\omega v_{cd}$$

$$(9) \quad v_{d}^* = P_c(s)(i_{d}^* - i_d) - L\omega i_{lq} + v_{cd}^*$$

$$(10) \quad v_{q}^* = P_c(s)(i_{q}^* - i_q) + L\omega i_{ld} + v_{cq}^*$$

The transfer functions $P_v(s) = K_{Pv} + \frac{K_{Iv}}{s}$ and $P_c(s) = K_{Pc} + \frac{K_{Ic}}{s}$ regulate the voltage and current control loops, respectively.

Droop Control

The performance of droop control structures for active and reactive power demands was investigated under nonlinear DG plug-and-play. When the inverter output is instantaneous, absolute power is essential for applying droop control laws. A low-pass filter with a fixed cutoff frequency is needed to get absolute power.

P, Q stand for absolute power and \tilde{p}, \tilde{q} denote instantaneous power, active and reactive, respectively. Conventional Droop is one of the most widely applied droop controllers. That includes m_p and n_q droop coefficients, ω is the system frequency, and V_n is the nominal voltage.

As for droop control with two integrators, there is an addition at both levels; as the control name, it has two integrators, one at the frequency level and the second at the voltage level.

Its Control laws are written in dq frame as follows:

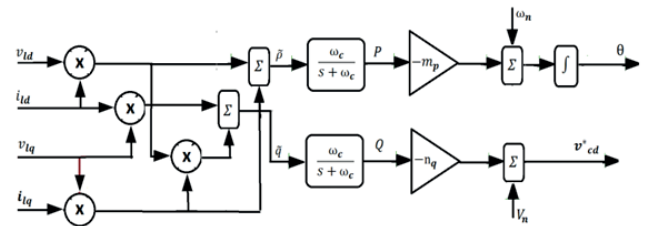


Fig. 2. Conventional droop control block diagram. [8]

$$(11) \quad \omega_i = \omega_0 - m_{pi} P_i$$

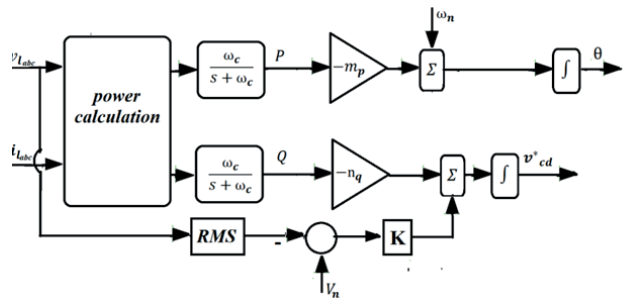


Fig. 3. Block diagram of a droop control with two integrators.

$$(12) \quad V_{cdi}^* = \tilde{E}_i = K(V_n - V_{di}) - n_{qi} Q_i$$

Where: $V_{cqi}^* = V_{lqi} = 0; V_{ni} = E_i$

Proposed Microgrid Solution

In the earlier research, the power-sharing at each DG output was regulated using droop control with two integrators. However, more is needed when addressing the varying loads and energy changes. Droop control with two integrators adjusts the output voltage or frequency based on power demand, but it has limitations in handling supply–demand variations and maintaining stability under dynamic conditions. PI control reduces oscillations and maintains a steady power supply, but it has limitations in dealing with transient modes and island mode operation. Despite these limitations, existing solutions can be improved by using the proposed solution based on IDA–PBC.

Port Hamilton strategy

The Port Hamilton (PH) model was proposed to simulate this system, where the PH framework guides developing and examining control rules that support stability and the intended energy-related behaviors. It also represents the system's total energy.

$$(13) \quad \frac{d(x)}{dt} = [J(x) - R(x)]\nabla H(x) + g(x)u + d$$

The state vector is x , and the control input vector is u . The antisymmetric interconnect matrix is denoted as $J(x)$, and $R(x)$ denotes the symmetric dissipation matrix, which reflects the internal losses of the system. $H(x)$ represents the Hamiltonian function quantifying the system's energy. $g(x)$ is the input matrix that depicts the system's connection port with the outside and defines the energy flow, and d is the vector of the external disturbances. The paper [9] and [10] contains additional information.

The main objective is to provide an improved method to overcome droop control with two integrators' limitations and achieve power-sharing precision. The suggested control consists of two parts modelled on the PH framework:

- **Voltage source inverter based on the PH**

VSI generates reference inverter voltages, which are required for distributed generation. Both controls were designed to attenuate the output filter.

$$(14) \quad \begin{bmatrix} L_i \frac{di_{di}}{dt} \\ L_i \frac{di_{qi}}{dt} \\ C_i \frac{dv_{cdi}}{dt} \\ C_i \frac{dv_{cqi}}{dt} \end{bmatrix} = \begin{bmatrix} 0 & \omega_i L_i & -1 & 0 \\ -\omega_i L_i & 0 & 0 & -1 \\ 1 & 0 & 0 & \omega_i C_i \\ 0 & 1 & -\omega_i C_i & 0 \end{bmatrix} \begin{bmatrix} i_{di} \\ i_{qi} \\ v_{cdi} \\ v_{cqi} \end{bmatrix} + \begin{bmatrix} 1 & 0 & 0 & 0 \\ 0 & 1 & 0 & 0 \\ 0 & 0 & -1 & 0 \\ 0 & 0 & 0 & -1 \end{bmatrix} \begin{bmatrix} v_{di} \\ v_{qi} \\ i_{ldi} \\ i_{lqi} \end{bmatrix}$$

- **Port-Hamiltonian-Based Droop Control with Two Integrators**

The new formula of the proposed control includes droop control with two integrators based on IDA-PBC to guarantee the decoupling between the reactive and active power and guarantee stability, where: $V_n = E_i; V_{ld} = E_0; a_0 = 1; a_1 = 1/K$

$$(15) \quad \begin{bmatrix} a_0 \frac{d\omega_i}{dt} \\ 1/K \frac{dE_i}{dt} \end{bmatrix} = \begin{bmatrix} 1 & 0 \\ 0 & 1 \end{bmatrix} \begin{bmatrix} \omega_i \\ E_i \end{bmatrix} + \begin{bmatrix} -m_{pi} & 0 \\ 0 & -n_{qi}/K \end{bmatrix} \begin{bmatrix} P_i \\ Q_i \end{bmatrix} + \begin{bmatrix} 0 \\ E_0 \end{bmatrix}$$

The Hamiltonian function representing the total energy of the system can be formulated as:

$$(16) \quad H_i(x) = \frac{1}{2} x_i^T F_i^{-1} x_i$$

$$x_i = \begin{bmatrix} x_{1i} & x_{2i} & x_{3i} & x_{4i} & x_{5i} \end{bmatrix}$$

$$F_i = \begin{bmatrix} i_{di} & i_{qi} & v_{cdi} & v_{cqi} & E_i \end{bmatrix}$$

And F_i is given by:

$$(17) \quad H_i(x_i) = \frac{1}{2L_i} x_{1i}^2 + \frac{1}{2L_i} x_{2i}^2 + \frac{1}{C_i} x_{3i}^2 + \frac{1}{C_i} x_{4i}^2 + \frac{1}{a_{1i}} x_{5i}^2$$

$$(18) \quad H_i(x_i) = \frac{1}{2} L_i i_{di}^2 + \frac{1}{2} L_i i_{qi}^2 + \frac{1}{2} C_i v_{cdi}^2 + \frac{1}{2} C_i v_{cqi}^2 + \frac{1}{2} a_{1i} E_i^2$$

Model for Closed-Loop System Based on IDA-PBC

In step two, the IDA-PBC control law will be calculated and implemented. These characteristics facilitate the synthesis of control laws to ensure stability. The IDA-PBC approach for a closed loop is represented as follows:

$$(19) \quad \frac{d(x)}{dt} = [J_d(x) - R_d(x)]\nabla H_d(x)$$

The essential components of the structure's preservation and integrability to meet the condition of stability are shown below:

$$(20) \quad R_{di}(x_i) = R_{di}^T(x_i) = \begin{bmatrix} A_1 & 0 & 0 & 0 & 0 \\ 0 & A_2 & 0 & 0 & 0 \\ 0 & 0 & A_3 & 0 & 0 \\ 0 & 0 & 0 & A_4 & 0 \\ 0 & 0 & 0 & 0 & A_{55} \end{bmatrix}$$

$$(21) \quad J_{di}(x_i) = -J_{di}^T(x_i) = \begin{bmatrix} 0 & 0 & -1 & 0 & 0 \\ 0 & 0 & 0 & -1 & 0 \\ 1 & 0 & 0 & 0 & 0 \\ 0 & 1 & 0 & 0 & 0 \\ 0 & 0 & 0 & 0 & 0 \end{bmatrix}$$

$$(22) \quad \nabla H_d(x) = \begin{bmatrix} i_{di} - i_{di}^* \\ i_{qi} - i_{qi}^* \\ v_{cdi} - v_{cdi}^* \\ v_{cqi} - v_{cqi}^* \\ E_i - E_i^* \end{bmatrix}$$

Equations (35 and (36) are dedicated to primary control objectives, including frequency synchronization, voltage regulation, and power-sharing. where: $E_i = V_n; E_0 = V_{ld}$.

Stability Verification

Hd (x) should have a minimum at equilibrium point x^* to achieve closed-loop stability and convergence under three conditions [13–15]:

$$(37) \quad \frac{\partial H_{ai}(x_i^*, x_i)}{\partial x_i} = \frac{\partial (H_{di}(x_i^*, x_i) - H_i(x_i^*))}{\partial x_i} \\ = \left[-\frac{1}{L_i} x_{1i}^*, -\frac{1}{L_i} x_{2i}^*, -\frac{1}{C_i} x_{3i}^*, -\frac{1}{C_i} x_{4i}^*, -\frac{1}{a_{1i}} x_{5i}^* \right]^T$$

$\partial H_{ai}(x_i^*, x_i)$ denotes the energy stored within the error terms of the controller.

$$(38) \quad \nabla H_i(x_i^*) = \frac{\partial H_i(x_i^*)}{\partial x_i} \\ = \left[\frac{1}{L_i} x_{1i}^*, \frac{1}{L_i} x_{2i}^*, \frac{1}{C_i} x_{3i}^*, \frac{1}{C_i} x_{4i}^*, \frac{1}{a_{1i}} x_{5i}^* \right]^T$$

$$(39) \quad \frac{\partial H_{di}(x_i^*)}{\partial x_i} = \frac{\partial H_{ai}(x_i^*, x_i)}{\partial x_i} + \frac{\partial H_i(x_i^*)}{\partial x_i} \\ = [0, 0, 0, 0, 0]$$

Condition 2:

$$(40) \quad \frac{\partial^2 H_{di}(x_i^*)}{\partial x_i^2} = \left[\frac{2}{L_i} + \frac{2}{C_i} + \frac{1}{a_{1i}} \right] > 0$$

Condition 3:

$$(41) \quad - \left[\frac{\partial H_{di}(x_i^*)}{\partial x_i} \right]^T R_{di} \frac{\partial H_{di}(x_i^*)}{\partial x_i} \\ = \begin{bmatrix} -\frac{a_{11}}{L_i} (x_{1i} - x_{1i}^*)^2 \\ -\frac{a_{22}}{L_i} (x_{2i} - x_{2i}^*)^2 \\ -\frac{a_{33}}{C_i} (x_{3i} - x_{3i}^*)^2 \\ -\frac{a_{44}}{C_i} (x_{4i} - x_{4i}^*)^2 \\ -\frac{a_{55}}{a_{1i}} (x_{5i} - x_{5i}^*)^2 \end{bmatrix}$$

The condition is verified when $a_{ii} \geq 0$
This study fulfilled all three conditions.

Simulation Results

This study compares previous method: droop control with two integrators, and the proposed Approach: droop control with two integrators based on IDA–PBC, in microgrid contains two DGs two impedance lines also load and step load. Both inverters will have the same control structures

The two inverters are considered identical. The controls have the same values. In addition, the step load can be controlled with a circuit breaker (CB) in 0.1 seconds. A simulation was conducted by building a microgrid model in MATLAB Simulink to confirm the suggested strategy's viability and efficacy. Where balanced Load1 is: P=64 Kw, Q=200 Var; Unbalanced Load2 is: $L_1=1\text{mH}$ $r_1=100\Omega$, $L_2=10\text{mH}$ $r_2=150\Omega$, $L_3=200\text{mH}$ $r_3=250\Omega$; nonlinear Load3 is: a Full bridge rectifier with RC load in parallel, $C_4=3.25\mu\text{F}$ $r_4=200\Omega$ and Step Load is: P= 25 Kw, Q=200 Var.

A simulated microgrid system was evaluated across several impedance lines. This section presents a comparison of two approaches over multiple impedance lines for six situations, as seen in the table below.

- Case one:

Figures (A) and (B) compare the previous approach's active and reactive power outputs and the proposed method.

Table 1. Power and controller parameters.

Parameters	Symbol	Values
Voltage source	V_{dc}	400V
Switching frequency	f_{sw}	10 KHz
Filter inductor	L	1.35 mH
Filter capacitor	C	50 μF
cutoff frequency	ω_c	31.41 rad/sec
Voltage per phase RMS	V_n	380 V
Phase	f_n	50 Hz
Frequency droop coefficient	m_p	$7e-5$ rad/(w*s)
Voltage droop coefficient	n_q	$5e-6$ V/var
Gain of Current (IDA–PBC)	$A_1; A_2$	50; 50
Gain of Voltage (IDA–PBC)	$A_3; A_4; A_{55}$	0.8; 0.8; 1
Gain of the integrator	K	10

Table 2. Various cases study for power sharing controls.

Case	Impedance lines
(a)	Resistor
(b)	Inductance
(c)	1.35 mH

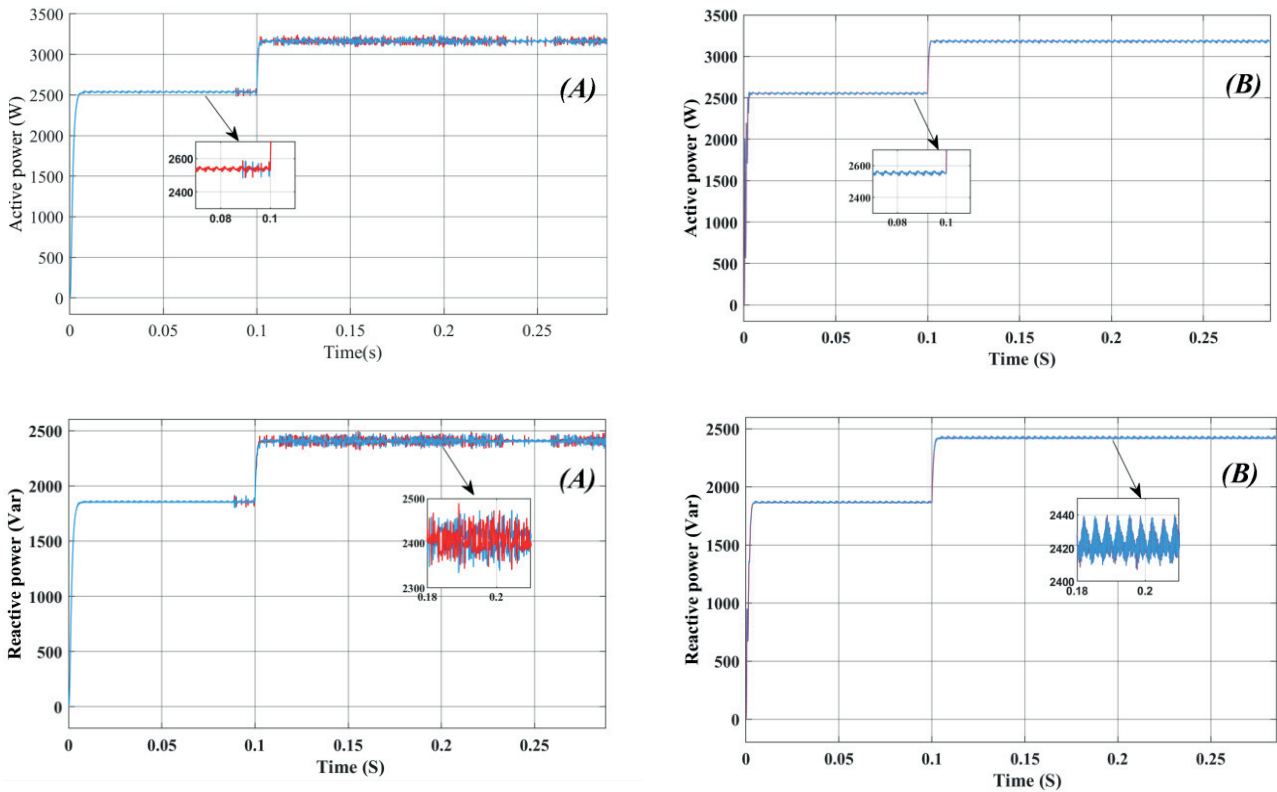


Fig. 6. Power outputs of distributed generators for resistor as impedance lines.

Each figure includes two distinct curves representing the power outputs of the two distributed generators (DGs): the red curve corresponds to DG1, while the blue curve corresponds to DG2. These curves offer a clear visualization of the performance and behavior of the system under the two methods.

When the DGs' resistances are assumed to be identical, a significant performance difference between the two approaches becomes evident. In the previous approach, the system failed to maintain stability when subjected to a step load injection at 0.1 seconds. The findings clearly suggest that the proposed strategy delivers a considerable increase in resilience and reliability compared to the old method.

- Case two

The figures below show that the preceding approach demonstrates instability in the succeeding 0.2 when utilizing inductances. Conversely, the proposed approach preserves consistency. This stability underscores the recommended method's greater flexibility and control capabilities, making it a more trustworthy alternative for systems.

- Case three

In case three, using a resistor and inductors together will make the power output of DG one and DG two more clearly identical when using the proposed method. After several changes in the impedance lines, it can be stated that the proposed method is more robust and performs better than the previous one across these different scenarios. With this model, further development can be made to better address most consumer problems of electrical flows in isolated areas.

Conclusion

This work has concentrated on developing grid-forming controllers in primary and internal control domains. It has underscored the limits of earlier control approaches and introduced a fresh approach – droop control with enhanced adaptive virtual impedance based on IDA-PBC. The work has given excellent results through comparative analysis with the latest droop control. The proposed technique has shown exceptional flexibility to changes in the microgrid system, effectively managing computational mistakes, noise, and disruptions. It has allowed precise proportional active power sharing and demonstrated resilience against parameter drift. While the simulation results in MATLAB demonstrate various advantages, a downside occurs in each injection starter, whether a distributed generator or a load. The purpose of future investigations is to improve this limitation. The insights gained from this study substantially contribute to the ongoing development of efficient control systems for inverter-based generators, fostering advancement in microgrid technologies.

Authors: PhD. Zakaria Charfi, Laboratory of Research in Electrotechnics and Automation, Medea, Algeria, E-mail: charfi.zakaria@univ-medea.dz; dr. Smain Bentouati, Laboratory of Mechanics, Physics, and Mathematical Modelling, Medea, Algeria, E-mail: bentouati.smain@univ-medea.dz; dr. Abdelhalim TLEMÇANI, Laboratory of Research in Electrotechnics and Automation, Medea, Algeria, University, E-mail: tlemcni.abdelhalim@univ-medea.dz.

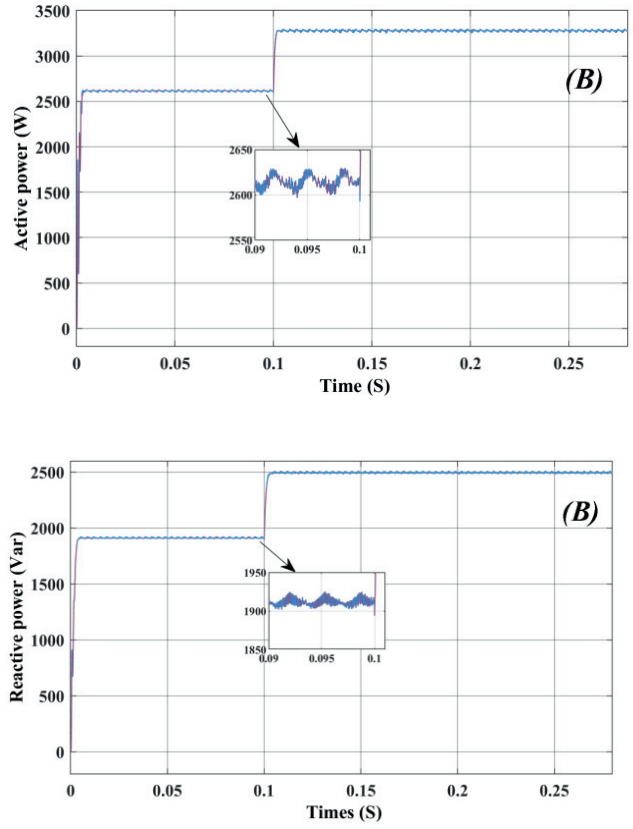
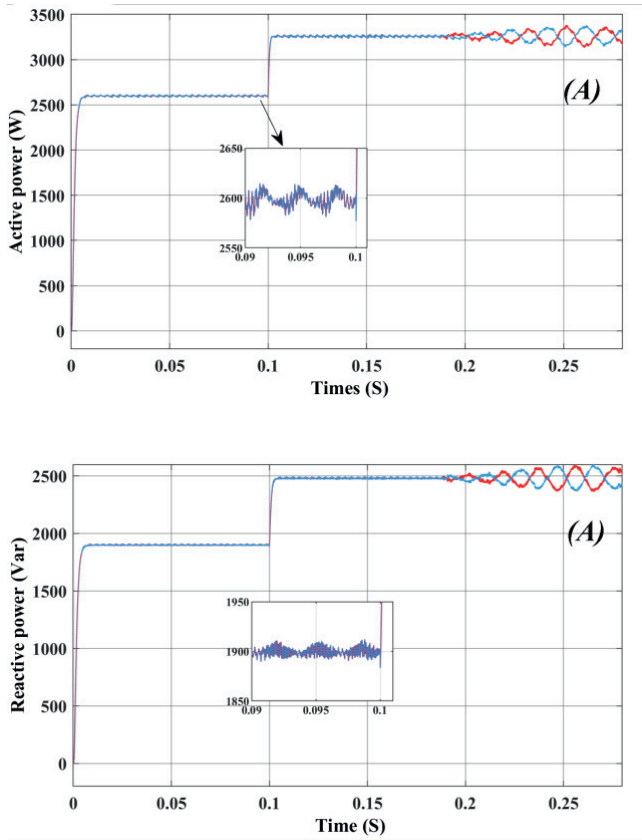


Fig. 7. Power outputs of distributed generators for inductance as impedance lines

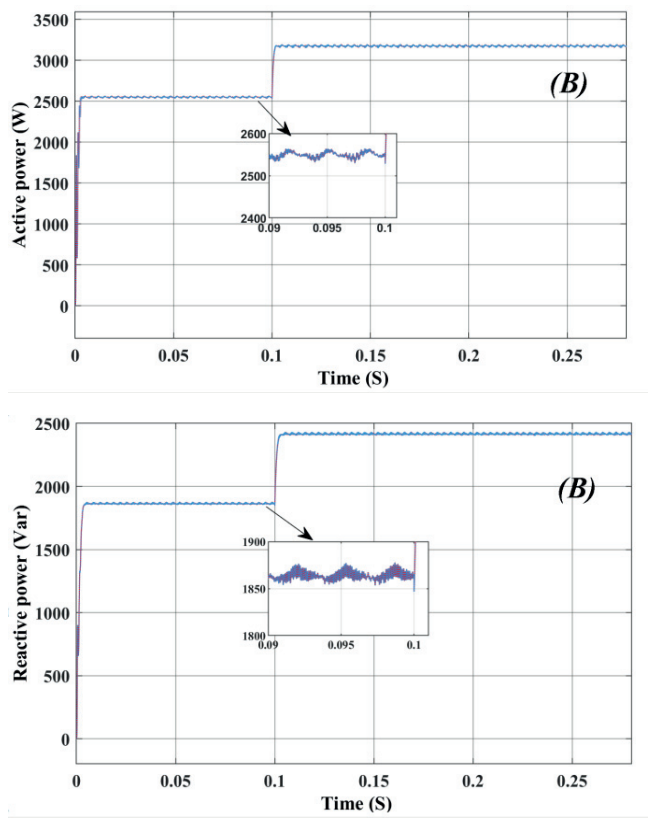
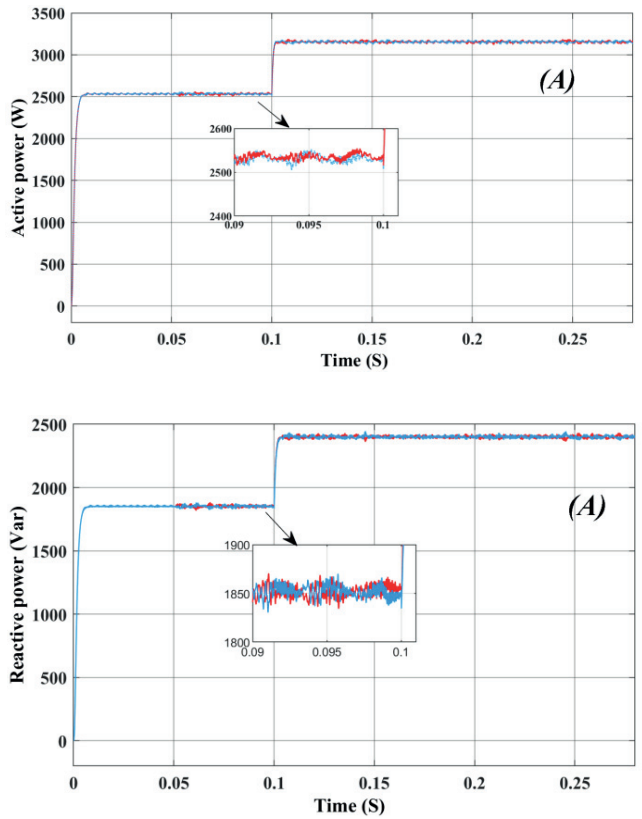


Fig. 8. Power outputs of distributed generators for impedance line containing resistance and inductance

REFERENCES

- [1] BOUDGHENE STAMBOULI, A., OULD AHMED, A. Design and optimization of a hybrid microgrid for remote areas in southern Algeria. *Journal of Renewable and Sustainable Energy*, v. 12, no. 1, 011201, 2020.
- [2] BAKHTIYAROV, A.; ABDULLAYEVA, G.; PIRIYEV, H. Analysis of electrical generators for wind and photovoltaic energy systems. *Przeegląd Elektrotechniczny*, v. 2024, n. 9, 2024.
- [3] REY, J. M.; JIMÉNEZ-VARGAS, I.; VERGARA, P. P.; OSMA-PINTO, G.; SOLANO, J. Sizing of an autonomous microgrid considering droop control. *International Journal of Electrical Power & Energy Systems*, v. 136, p. 107634, 2022.
- [4] DHEER, D. K.; GUPTA, Y.; DOOLLA, S. A self-adjusting droop control strategy to improve reactive power sharing in islanded microgrid. *IEEE Transactions on Sustainable Energy*, v. 11, n. 3, p. 1624–1635, 2019.
- [5] CHARFI, Z.; BENTOUATI, S.; TLEMCANI, A. A comparison of control strategies for passivity-based VSI in microgrids between conventional droop control and droop control with two integrators. In: *2nd International Conference on Electronics, Energy and Measurement (IC2EM)*, 2023.
- [6] KHEFIFI, N.; HOUARI, A.; MACHMOUM, M.; SAIM, A.; GHANES, M. Generalized IDA-PBC control using enhanced decoupled power sharing for parallel distributed generators in standalone microgrids. *IEEE Journal of Emerging and Selected Topics in Power Electronics*, v. 9, n. 4, p. 5069–5082, 2020.
- [7] GERVASIO, F. A.; BUENO, E.; MASTROMAURO, R. A.; LISERRE, M.; STASI, S. Voltage control of microgrid systems based on 3LNPC inverters with LCL-filter in islanding operation. In: *International Conference on Renewable Energy Research and Applications (ICRERA)*, 2015.
- [8] CHARFI, Z.; BENTOUATI, S.; TLEMCANI, A. Two-stage converter based on droop control and IDA-PBC in islanded mode. In: *International Conference on Advances in Electronics, Control and Communication Systems (ICAEECS)*, 2023.
- [9] GUPTA, Y.; CHATTERJEE, K.; DOOLLA, S. Controller design, analysis, and testing of a three-phase VSI using IDA-PBC approach. *IET Power Electronics*, v. 13, n. 2, p. 346–355, 2020.
- [10] ORTEGA, R.; VAN DER SCHAFT, A.; MASCHKE, B.; ESCOBAR, G. Interconnection and damping assignment passivity-based control of port-controlled Hamiltonian systems. *Automatica*, v. 38, n. 4, p. 585–596, 2002.
- [11] DHEER, K.; SONI, N.; DOOLLA, S. Improvement of small signal stability margin and transient response in inverter-dominated microgrids. *Sustainable Energy, Grids and Networks*, v. 5, p. 135–147, 2016.
- [12] LU, M.; DUTTA, S.; PURBA, V.; DHOPLA, S.; JOHNSON, B. A grid-compatible virtual oscillator controller: Analysis and design. In *Proc. IEEE Energy Conversion Congress and Exposition (ECCE)*, Baltimore, MD, USA, 2019.
- [13] ORTEGA, R.; VAN DER SCHAFT, A.; MASCHKE, B.; ESCOBAR, G. Interconnection and damping assignment passivity-based control of port-controlled Hamiltonian systems. *Automatica*, v. 38, no. 4, 2002.
- [14] ORTEGA, R.; GARCIA-CANSECO, E. Interconnection and damping assignment passivity-based control: Towards a constructive procedure – Part I. In *Proc. 43rd IEEE Conference on Decision and Control (CDC)*, Nassau, Bahamas, 2004.
- [15] GARCIA-CANSECO, E.; ASTOLFI, A.; ORTEGA, R. Interconnection and damping assignment passivity-based control: Towards a constructive procedure – Part II. In *Proc. 43rd IEEE Conference on Decision and Control (CDC)*, Nassau, Bahamas, 2004.